Teaching Apparatus for Differential Pressure Flow Sensor Based on Graphene Film F-B Cavity

Huichao Shi*, Qingyang Wang, Zhaojie Kou and Yiwen Wang

College of Information Science and Technology, Beijing University of Chemical Technology, Beijing, China
* Corresponding author: Huichao Shi

Abstract: In order to enable students to have a deeper understanding of the working principle, signal conversion, and signal processing of the graphene film F-B cavity, authors designed and manufactured a differential pressure flow sensor based on the graphene film F-B cavity from the perspective of practical application. And a water flow calibration experimental and optical signal detection experimental platform were built, from the perspective of classroom teaching demonstration of the undergraduate course "Sensor Principle", combining the flow sensor with calibration device to form a teaching apparatus. The measurement process and calibration process of the designed flow sensor is fully demonstrated to help students gain a deeper understanding of the working principle and calibration requirement of the flow sensor. The calibration experiment shows that the teaching apparatus can fully and vividly demonstrate the working principle and measurement process of the differential pressure flow sensor based on the graphene film F-B cavity, and achieve good experimental teaching results.

Keywords: Differential pressure flow sensor; Graphene film F-B cavity; Working mechanism; Teaching apparatus.

1. Introduction

As an important teaching content of the undergraduate professional course "Sensor Principles", fiber optic F-B cavity based on graphene film have been widely used in various sensors due to their simple structure, high sensitivity, and good dynamic response[1-3]. At present, sensors using graphene film F-B cavities as sensing elements have been widely used in various fields such as pressure measurement[4-6], underwater acoustic measurement[7-8], gas concentration measurement[9-10], atmospheric humidity measurement[11-12], and other measurements[13-14]. This device is a sensitive structure that can be integrated into various types of high-precision sensors [15-16]. Meanwhile, the graphene film F-B cavity is an optically sensitive structure that outputs optical signal and can be transmitted over long distances through optical fiber. Therefore, for many practical measurement occasions that are not suitable for outputting electrical signals (such as explosion-proof areas), this type of sensitive structure has great application potential.

However, due to students lack of experience in designing sensor sensitive structures and limited exposure to practical engineering problems, their understanding of the sensor design and working principle of graphene film F-P cavity as sensitive structure, as well as their understanding of specific measured applications, is not deep enough, which to some extent affects the teaching effectiveness.

In this paper, the author designed and manufactured a differential pressure flow sensor based on the graphene film F-P cavity, built a water flow calibration platform and optical signal detection experimental platform, which could fully demonstrate the measurement process of a differential pressure flow sensor based on the graphene film F-P cavity. By studying the working principle, design concept, and classroom demonstration experiments of this sensor, students' understanding of this type of sensor has been deepened, and the goal of combining classroom teaching with engineering practice has been achieved.

2. Working Principle

2.1. Working Principle of Fiber F-P Cavity Based on Graphene Film

The fiber F-P cavity based on the graphene film is shown in Figure 1, and its working principle is shown in Figure 2. The graphene film is used as the reflective film of the F-P cavity end face. After the light beam is refracted from the fiber end face into the F-P cavity, the refraction and reflection occur at the graphene film, and the reflected light beam occurs in the same process at the fiber end face to form a multi-beam interference signal output.

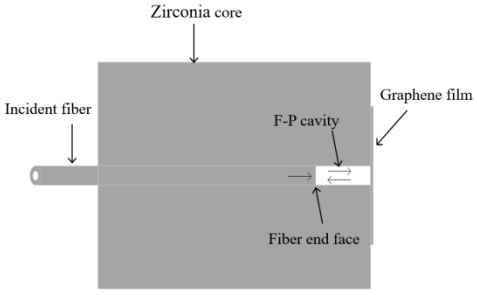

Figure 1. Optical path diagram of F-P cavity

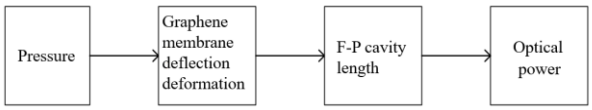

Figure 2. Measurement mechanism of graphene membrane F-P cavity

When the optical power of the incident light is I_0, the optical path difference between two beams is δ is

$$\delta = 2nlcos\theta_1 \quad (1)$$

In the Eq. (1), n is the refractive index of the medium in the F-P cavity, and the medium in the cavity is air, then n=1.00029. l is the F-P cavity length. θ_1 is the incident angle of the incident light.

Let the phase difference be φ and λ is the wavelength of the incident light, so the phase difference between two beams is

$$\varphi = 2\pi\frac{\delta}{\lambda} = 4\pi\frac{nlcos\theta_1}{\lambda} \quad (2)$$

When the light is incident perpendicular to the graphene membrane, the phase difference φ could be expressed as the following formula [17-18].

$$\varphi = \frac{4\pi nl}{\lambda} \quad (3)$$

Because a monochromatic light source is used as the input light source in this paper, and its wavelength λ is a fixed value, it can be received directly by the optical power meter without considering the change of wavelength, and the power signal received by the optical power meter can be simplified as [17-18]

$$I_R = \frac{R_1+\xi R_2-2\sqrt{\xi R_1 R_2}cos\varphi}{1+\xi R_1 R_2-22\sqrt{\xi R_1 R_2}cos\varphi} I_0 \quad (4)$$

In the Eq. (4), I_R is the reflected light power. R_1 and R_2 are the optical reflectance of the fiber end face of the F-P cavity and the graphene film, respectively. The value of R_1 is 0.02, and the value of R_2 is about 0.01, which are determined by the graphene film characteristic matrix. ξ is the coupling coefficient of F-P cavity length.

By substituting Eq. (3) into Eq. (4), the mathematical formula of reflected light power and F-P cavity length can be obtained

$$I_R = \frac{R_1+\xi R_2-2\sqrt{\xi R_1 R_2}cos\frac{4\pi nl}{\lambda}}{1+\xi R_1 R_2-22\sqrt{\xi R_1 R_2}cos\frac{4\pi nl}{\lambda}} I_0 \quad (5)$$

2.2. Working Principle of the Differential Pressure Flow Sensor

The differential pressure flow sensor is composed of a pressure-sensitive structure of graphene film F-P cavity and a microfluidic chip. The measurement principle is: when the liquid flows through the flow channel of the microfluidic chip, it will bring pressure difference to the pressure sensitive structure of the graphene film F-P cavity upstream and downstream of the flow channel, and the change of different pressure of the upstream and downstream will lead to different reflected light power, that is, the optical power difference. Because the pressure loss along the pipeline is related to the flow rate, so the optical power difference is related to the flow rate. Therefore, the output optical power of the pressure sensitive structure of the graphene film F-P cavity in the upstream and downstream flow channels can be collected by an optical power meter, and the flow rate can be measured by the corresponding relationship between the optical power difference and the flow rate. The differential pressure flow sensor based on above principle is shown in Figure 3.

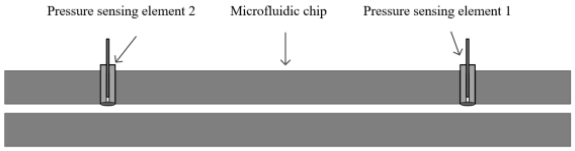

Figure 3. Design diagram of differential pressure flow sensor

The differential pressure flow sensor is suitable for laminar flow, where the fluid is incompressible water, because the size of the flow channel is very small [19]. The pressure loss of incompressible fluid flowing along a circular straight pipe in laminar flow state can be expressed by the Hagen-Poiseuille formula,the formula is shown as

$$\Delta p = \frac{128\mu QL}{\pi D^4} \quad (6)$$

In the Eq. (6), D is the diameter of the circular straight pipe. Q is the volume flow rate of the fluid. μ is the dynamic viscosity of fluid;. L is the length of the pipe between the pressure measuring points.

The measuring principle of differential pressure flowmeter is relatively simple, as long as the pressure difference between the upstream and downstream fluid of the pipeline is measured, the flow information can be obtained through calculation. Flow rate can be calculated by substituting differential pressure data into Eq. (7), as shown

$$Q = \frac{\pi D^4}{128\mu L}\Delta p \quad (7)$$

The flow channel of the designed microfluidic chip is a rectangular channel with a square cross section. Then the relationship between flow rate and differential pressure along the rectangular pipeline can be expressed by

$$Q = \frac{D^4}{32\mu L}\Delta p \quad (8)$$

In the Eq. (8), D is the side length of the square section of the rectangular pipeline. Q is the volume flow rate of the fluid. μ is the dynamic viscosity of fluid. L is the length of the pipe between the pressure measuring points.

2.3. Sensor Structure Design

The differential pressure flow sensor is composed of two pressure-sensitive structure of graphene membrane F-P cavity and a microfluidic chip. The sensitive structure and fabrication of graphene film F-P cavity is shown in Figure 4.

Firstly, the pressure-sensitive structure of the graphene membrane F-P cavity is fabricated. The graphene film used in the production came from Nanjing Jicang Nano Technology Co., LTD., and it was made by chemical vapor deposition (CVD). The total film number was 10 layers. The graphene film is adsorbed on the end face of the zirconia core due to the intermolecular van der Waals force. The peeled and cut optical fiber is clamped on a 3D mobile platform and inserted into the inner diameter of the

zirconia core with the help of the 3D mobile platform, so that the end face of the optical fiber and the graphene film form an F-P cavity, and the length of the F-P cavity is pushed into the appropriate length, so that the F-P cavity length meets the experimental requirements.

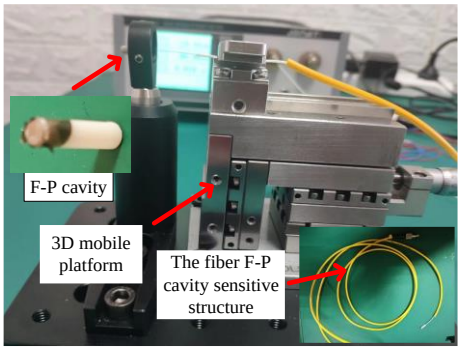

Figure 4. The sensitive structure and fabrication of graphene film F-P cavity

The completed differential pressure flow sensor is shown in Figure 5. The size of the microfluidic chip is 25mm*80mm, the length of the flow channel is 70mm, the section size of the flow channel is 0.125mm, and the distance between the two pressure sensitive structures of F-P cavity is 30mm. The microfluidic chip is multi-layer Mosaic, made of PDMS material.

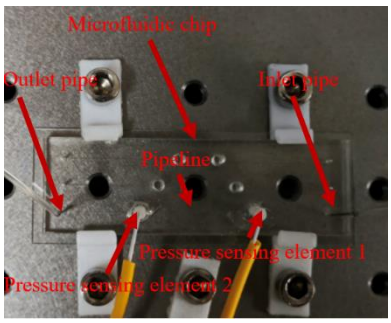

Figure 5. Experimental sample diagram of differential pressure flow sensor

3. Experimental Platform

The real flow experiment platform includes injection pump, syringe, plastic hose, differential pressure flow sensor, optical power meter, electronic balance and acquisition program. The injection pump is used for the main water supply of the microfluidic chip, and the flow rate can be controlled with different syringes. Figure 6 shows the experimental platform.

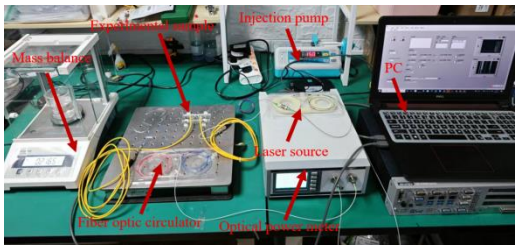

Figure 6. Real flow experimental platform

The injection pump is used for the main water supply of the microfluidic chip. The injection pump used in this experimental platform is Lande medical injection pump, which has high design integration, simple operation, small volume and light quality. Table 1 lists the main parameters of the injection pump.

Table 1. Main parameters of the injection pump

Project	Major parameter
Syringe	10mL,20mL,30mL,50mL
Flow range	0.1mL/h~-300mL/h(10mL) 0.1mL/h~-600mL/h(20mL) 0.1mL/h~-800mL/h(30mL) 0.1mL/h~-1200mL/h(50mL)
Flow accuracy	±2%
Setprecision	0.1mL/h
Occlusion pressure	40kPa~70kPa(8 levels in total）

The standard flow rate can be calculated using a weighing balance. High precision electromagnetic force balance sensor used in this experimental platform. The accuracy of the measurement results is higher, the response speed is faster, and the fault is less. The main parameters of the electronic balance used are shown in Table 2.

Table 2. The main parameters of the electronic balance

Project	Technical index
model	FA2204EN
range	220 g
Minimum weighing	0.01g
reading accuracy	0.0001g

4. Experimental Testing

The actual flow experiment process is as follows.

The 1550nm laser light source channel 1 is connected to the A connector of the three-port ringer 1, the fiber connector of the fiber F-P cavity sensitive structure upstream of the microfluidic chip is connected to the B connector of the three-port ringer 1, and the C connector of the three-port ringer is connected to the channel 1 of the optical power meter. The laser light source channel 2 is connected to the A connector of the three-port ringer 2, connecting the fiber optic connector of the fiber F-P cavity pressure sensing element downstream of the microfluidic chip to the B connector of the three-port ringer 2, and connecting the C connector of the three-port ringer 2 to the channel 2 of the optical power meter.

The plastic hose connects the inlet of the microfluidic chip flow channel to the syringe on the injection pump, and the outlet of the microfluidic chip flow channel is connected to the wastewater beaker through the plastic hose.

RS232 is used to connect the optical power meter to the computer, and the optical power acquisition program transfers the data of the optical power meter to the computer. The acquisition frequency remains at the default 50KSPS, and the measurement time is 60 seconds. The data collected by the acquisition software is saved in Excel.

Due to differences in sample production, the optical power output of the two sensitive structures varies under the same flow rate. Therefore, the optical power at a flow rate of 0mL/min is collected, and the measured data at other flow points are normalized based on the optical

power at a flow rate of 0mL/min. The optical power of channels CH1 and CH2 collected are shown in Table 3.

Table 3. Dual-channel optical power collected for flow experiments

Flow rate	CH1 Average optical power	CH2 Average optical power	Difference(CH1 and CH2)	Normalized optical power difference
mL/min	dBm	dBm	dBm	dBm
0	-11.42	-17.49	6.07	0.00
0.05	-11.15	-15.66	4.52	-1.55
0.10	-11.46	-17.13	5.67	-0.40
0.15	-11.83	-19.50	7.66	1.60
0.20	-11.75	-17.72	5.97	-0.10
0.25	-12.38	-17.42	5.04	-1.03
0.30	-12.27	-16.76	4.49	-1.58
0.35	-12.14	-17.67	5.53	-0.53
0.40	-11.86	-19.57	7.71	1.64
0.45	-11.39	-17.02	5.63	-0.43
0.50	-11.05	-17.02	5.97	-0.10

According to the theoretical model between optical power and flow rate, the flow rate range 0.233~0.283 mL/min is selected. The collected data can only be analyzed after processing such as difference processing, SVD, and FFT transformation.

By substituting the set flow point into the theoretical model of optical power difference and flow rate, the calculated optical power difference under this flow point could be obtained. The standard flow rate is the set flow rate of the injection pump during the calibration experiment. The experimental data and theoretical model calculation data are shown in Table 4.

Table 4. Flow calibration experimental data and theoretical data

Standard flow rate	Experiment#1 Optical power difference	Experiment#2 Optical power difference	Experiment#3 Optical power difference	Theory Optical power difference
mL/min	dBm	dBm	dBm	dBm
0.233	5.16	4.88	5.04	4.60
0.242	3.39	4.35	3.33	3.75
0.250	2.86	3.73	2.31	2.71
0.258	1.74	1.49	1.18	1.57
0.267	-0.35	0.08	0.70	0.37
0.275	-1.30	-0.12	-1.29	-0.88
0.283	-1.52	-2.26	-2.48	-2.15

5. Conclusion

In this paper, the author designed and manufactured a differential pressure flow sensor based on the graphene film F-P cavity, built a water flow calibration experimental platform and optical signal detection experimental platform, which could fully demonstrate the measurement process of a differential pressure flow sensor based on the graphene film F-P cavity. This sensor can be used for classroom teaching demonstration of "Sensor Principle", which not only enables students to understand the working principle, signal conversion, and signal processing of the sensor, but also has an understanding of the design method, testing method, and data processing process of the sensor sensitive structure, in order to achieve the goal of combining classroom teaching with engineering practice. The experimental results also show that the sensor can effectively measure liquid flow.

References

[1] Dong N, Wang S, Jiang L, et al. Pressure and temperature sensor based on graphene diaphragm and fiber Bragg gratings. IEEE Photonics Technology Letters, 2017, Volume 30, pp. 431-434.

[2] Li L, Feng Z, Qiao X, et al. Ultrahigh sensitive temperature sensor based on Fabry–Pérot interference assisted by a graphene diaphragm. IEEE Sensors Journal, 2014, Volume 15, pp. 505-509.

[3] Li, C, Xiao, J, Guo, TT, Fan, SC, Jin, W. Interference characteristics in a Fabry – Perot cavity with graphene membrane for optical fiber pressure sensors (Article). Microsystem Technologies, 2015, Volume 21, pp. 2297-2306.

[4] Cheng L, Qianwen L, Tingting G, et al. An ultra-high sensitivity Fabry-Perot acoustic pressure sensor using a multilayer suspended graphene diaphragm, 2015 IEEE SENSORS. IEEE, 2015, pp. 1-4.

[5] Cui Q, Thakur P, Rablau C, et al. Miniature optical fiber pressure sensor with exfoliated graphene diaphragm. IEEE Sensors Journal, 2019, Volume 19, pp. 5621-5631.

[6] W. Ni et al. "Ultrathin graphene diaphragm-based extrinsic Fabry–Pérot interferometer for ultra-wideband fiber optic acoustic sensing", Opt. Express, 2018, Volume 26, pp. 20758-20767.

[7] Li C, Gao X, Guo T, et al. Analyzing the applicability of miniature ultra-high sensitivity Fabry–Perot acoustic sensor using a nanothick graphene diaphragm. Measurement Science and Technology, 2015, Volume 26, pp. 085101.

[8] Ma J, Xuan H, Ho H L, et al. Fiber-optic Fabry–Pérot acoustic sensor with multilayer graphene diaphragm. IEEE Photonics Technology Letters, 2013, Volume 25, pp. 932-935.

[9] Ma J, Zhou Y, Bai X, et al. High-sensitivity and fast-response fiber-tip Fabry–Pérot hydrogen sensor with suspended palladium-decorated grapheme. Nanoscale, 2019, Volume 11, pp. 15821-15827.

[10] Monteiro C S, Raposo M, Ribeiro P A, et al. Acoustic optical fiber sensor based on graphene oxide membrane. Sensors, 2021, Volume 21, pp. 2336.

[11] Cheng L,Xiyu Y,Tian L, et al. Insensitivity to Humidity in Fabry–Perot Sensor With Multilayer Graphene Diaphragm. IEEE Photonics Technology Letters, 2018, Volume 30.

[12] Li C, Yu X, Zhou W, et al. Ultrafast miniature fiber-tip Fabry–Perot humidity sensor with thin graphene oxide diaphragm. Optics letters, 2018, Volume 43, pp. 4719-4722.

[13] Zhang L, Huang Y, Niu X, et al. High-sensitivity fiber optic Fabry–Perot ultrasonic sensor based on a grooved silicon diaphragm for partial discharge detection. Applied Optics, 2023, Volume 62, pp. 6809-6815.

[14] Zhang W, Wang R, Rong Q, et al. An optical fiber Fabry-Perot interferometric sensor based on functionalized diaphragm for ultrasound detection and imaging. IEEE Photonics Journal, 2017, Volume 9, pp. 1-8.

[15] Li C, Lan T, Yu X, et al. Room-temperature pressure-induced optically-actuated Fabry-Perot nanomechanical resonator with multilayer graphene diaphragm in air. Nanomaterials, 2017, Volume 7, pp. 366.

[16] Wang S, Chen W. A large-area and nanoscale graphene oxide diaphragm-based extrinsic fiber-optic Fabry–Perot acoustic sensor applied for partial discharge detection in air. Nanomaterials, 2020, Volume 10, pp. 2312.

[17] Xiao X, Fan S C, Li C. The Effect of Edge Mode on Mass Sensing for Strained Graphene Resonators. Micromachines, 2021, Volume 12, pp. 189.

[18] Zhou X, Yu Q .Wide-Range Displacement Sensor Based on Fiber. Sensors Journal IEEE, 2011, Volume 11, pp. 1602-1606.

[19] Pfitzner J .Poiseuille and his law. Anaesthesia, 2010, Volume 31, pp. 273-275.